The potential use of torrefied Nigerian biomass for combustion applications

Femi S. Akinrinola, Nwigwudu Ikechukwu, Leilani. I. Darvell, Jenny M. Jones, Alan Williams*.

School of Chemical and Process Engineering, University of Leeds, LS2 9JT. UK

*Author to whom correspondence should be addressed: E-mail: a.williams@leeds.ac.uk

Abstract

Many countries are seeking to expand their use of solid biomass for electricity and heat generation. Nigeria, too, is exploring its own potential energy crops and indigenous residues. The use of this biomass for energy production is, however, limited by factors such as high moisture content, low bulk and low energy density. This study examines the torrefaction and combustion properties of four readily available Nigerian woody biomass, *Gmelina arborea, Terminalia superba*, *Nauclea diderrichii*, *Lophira alata* and a residue, palm kernel expeller (PKE). They are considered for their suitability for use in large scale power stations, especially as pulverized fuels.

The Fuels were torrefied at 270 and 290^{o}C for either 30 or 60 min, and assessed for pyrolysis and combustion characteristics in comparison to their untreated counterparts. Energy densities of the woods improved from 19.2-21.2 MJ/kg for the raw fuels to 21.5-24.6 MJ/kg for the torrefied fuels. The milling behaviour of the torrefied fuels improved upon torrefaction, especially for Nauclea; however, torrefaction had very little effect on the grindability of PKE. The apparent first order kinetics for pyrolysis were determined by thermogravimetric analysis (TGA). After torrefaction, the fuels become less reactive; *Nauclea* and *Gmelina* were the most reactive fuels, whilst PKE was the least reactive. The combustion behavior of selected fuels was visually examined in a methane air flame. This showed that torrefaction resulted in shorter ignition delay, shorter duration of volatile combustion and longer duration of char burn out.

Keywords: Nigeria; Biomass; Torrefaction, Pyrolysis; Combustion.

1.0 Introduction

Whilst the demand for sustainable heat and electricity generation continues to increase worldwide there is also a need to reduce carbon emissions globally [1]. In Africa there are a number of coal-fired power stations and plans to build more [2]; in Nigeria there is single coal fired power station that uses fluidized bed technology. But there is potential to build power stations using biomass or coal-biomass blends since this technology is widely recognized as a method to control carbon emissions [3-6]. Many Developing Nations rely on woody biomass to meet their basic energy needs, especially in rural areas and this is the case in Nigeria [3,4]. At present the amount of biomass used for large scale electricity generation is limited, but many studies have been made into the use of solid biomass fuels alone or co-fired with coal, for example [6-8]. Here we study four woods and an agricultural residue, Palm Kernel Expeller (PKE) all of which are widely available in Africa and Asia [3,4,9,10], Only a few studies have specifically considered the properties and use of torrefied Nigerian woody biomass [9,10].

Despite the abundance of bioenergy in Nigeria in the form of wood, straw and waste [3], there are problems associated with its use. Transportation and storage for biomass is difficult as a result of the low energy density and the high moisture content which also reduces the thermal efficiency for energy production. In pulverized fuel or some fluidised bed applications, the energy required for grinding to a suitable particle size due to its tenacious and fibrous nature is considerable. Torrefaction is a pre-treatment process that can reduce these problems [11-14]

].

Torrefaction involves the use of low temperature pyrolysis ranging between 200 and 300°C, in the absence of oxygen. The process causes the biomass to lose low molecular weight volatile compounds due to the decomposition of hemicellulose and the partial decomposition

of lignin [15-17]. About 70% of the initial biomass weight and about 90% of the original biomass energy is retained, resulting in energy densification, and it becomes more friable and easier to mill. The resultant solid fraction, i.e. the torrefied fuel, consists of some unreacted cellulose, unreacted lignin as well the as non-volatile byproducts of cellulose degradation.

Studies have been made of the reaction kinetics and combustion behaviour of raw and torrefied biomass [18-22]. These have shown the difference between coal and torrefied fuels [23] and the differences between the reactivities of raw and torrefied fuels [24,25]. The characteristics of a torrefied flame have been examined [26] and a CFD study made of the combustion of a torrefied wood in a combustor [27].

This paper examines the effect of torrefaction on four woods which are widely grown in Nigeria [10], but also in Africa generally and in Asia, and an agricultural residue, Palm Kernel Expeller (PKE). The effects on milling performance and on the fuel-nitrogen distribution were examined. Their combustion characteristics are compared to their raw, untreated, counterparts.

Experimental methods

2.1 Sample Preparation

Four Nigerian woody biomass namely *Gmelina arborea*, *Terminalia superba*, *Nauclea diderrichii*, *Lophira alata* and a residue, Palm Kernel Expeller (PKE), were studied. These fuels were supplied by Quintas Renewable Energy Solutions Limited, Nigeria in the form of chips. These fuels have been characterized previously [9].

For the combustion tests, the samples were cut into cubes of approx. 2mm x 2mm x 2mm. The samples used for the grindability test were milled using a Retsch Cutting Mill SM100 to obtain a size fraction <600-1180μm. The samples were further pulverized to a size <53μm using the Retsch Ball Mill PM100 for proximate, ultimate and thermogravimetric analyses.

2.2 Torrefaction Process

The torrefaction of the fuels was performed in 100g batches in a horizontal tube furnace with a reactor tube of internal diameter of 60 mm and 800 mm in length. Details of the reactor have been published previously [16, 28]. The reactor was heated at a rate of 10ºC /min from 30 ºC to the desired final temperature of either 270 or 290 ºC under a flow of nitrogen (1.2 L/min) and then kept at this temperature for the desired reaction time. The reaction time is defined as the time at which the sample spends at a temperature of 200ºC or above. When the reaction time was completed, the reactor tube was quenched under flowing nitrogen. The solid residue in the reactor was weighed and the mass yield was calculated as a percentage of the original dried mass sample, using equation 1. The corresponding energy yield was also calculated as a function of mass yield using equation 2 below.

$$\text{Mass yield, } h_M = \left(\frac{Mchar}{Mfeed}\right) \quad (1)$$

$$\text{Energy yield, } h_E = h_M \cdot \left(\frac{HHVchar}{HHVfeed}\right) \quad (2)$$

where M_{char} is the mass of the torrefied product, M_{feed} is the dry mass of the untreated biomass (both on a dry basis), HHV_{char} is the higher heating value of the torrefied biomass and HHV_{feed} is the higher heating value of the raw biomass, both also on a dry basis.

Table 1 lists the sample designation for the different fuels and torrefaction conditions applied in order to optimize mass and energy yields for the different fuels. From the samples torrefied at 270ºC for 30 min, PKE was the sample least affected by torrefaction and so additional measurement were made at 290ºC.

2.3 Fuel characterization

The moisture, volatile and ash contents were determined using the British Standards BS EN 14774-1:2009, BS EN 15148:2009 and BS EN 14775:2009, respectively. The fixed carbon content was measured by difference. An elemental analyzer (CE instruments Ltd, Flash EA 1112 Series) was used to determine the C, H and N contents of the solid. Measurements were performed in duplicate and a mean values reported. Oxygen was determined by difference. The high heating value of the fuels on a dry basis (HHV dry) were determined experimentally by the bomb calorimetric method according to DIN 51900 T3 standard. They were also estimated for comparison purposes from the ultimate analysis (dry basis) and using the correlation proposed by Friedl et al. [29] given in equation 3 [29]. The results agreed within ±0.2 MJ/kg.

$$HHV = 3.55\ C^2 - 232\ C - 2230\ H + 51.2C \times H + 131N + 20{,}600\ (kJ/kg) \quad (3)$$

The grindabilities of the fuels were determined using a modified form of the Hardgrove Grindability Index (HGI) method [30]. The coals and biomass samples were first sieved to obtain a fraction in the range of 600-1180μm. A fixed volume of 50 cm^3 of sieved sample was ground further in a Retsch PM100 ball mill for the prescribed time and then the particle size distribution determined. For the mill calibration, the percentage of the sample fraction that passed though the 75μm sieve was plotted against the HGI values for the reference coals and a linear fit of the resultant calibration (R2 = 0.97) was used to calculate the equivalent HGI of the biomass samples using equation (4).

$$HGI_{equiv} = \frac{m+0.8258}{0.1746} \quad (4)$$

where m is the percentage of biomass sample passing through 75 μm sieve.

For the particle size distribution plots, the samples from the HGI test was sieved using a stack of sieves of mesh sizes 600, 355, 212, 150, 75 and 53μm. The mass of sample retained on each sieve was measured and calculated as a percentage of the original mass sample.

Lignocellulose Analysis was undertaken as follows: The gravimetric measurements of Neutral Detergent Fibre (NDF), Acid Detergent Fibre (ADF) and Acid Detergent Lignin (ADL) were made using the Gerhardt fibrecap system, which is the improved version of Van Soest's methods [31, 32]. The NDF, which is regarded as the total cell wall is the residue, corrected for ash, left after refluxing for 1h in a neutral buffered detergent solution. ADF, the ash corrected residue remaining after refluxing the samples in a solution of cetyl ammonium bromide (CTAB) in 2 M sulphuric acid is a measure of cellulose and lignin only. ADL was measured by treating ADF with 72% sulphuric acid to solubilise the cellulose to determine crude lignin. Ash was determined in the samples after heating at 600°C in a muffle furnace for at least 4h. The concentration of hemicelluloses and cellulose were calculated by Equations (5) and (6) respectively.

$$\%\text{Hemicellulose} = \%\text{NDF} - \%\text{ADF} \quad (5)$$

$$\%\text{Cellulose} = \%\text{ADF} - \%\text{ADL} \quad (6)$$

2.6 Pyrolysis and combustion studies

The pyrolysis of fuels and char burning profiles were investigated using a TA Q5000 thermogravimetric analyser. For pyrolysis, a typical mass of ~3 mg of sample was heated at rate of 10°C /min to 700°C in a purge of nitrogen at a flow rate of 50 mL/min. This was followed by cooling to ~40°C before heating up again at 10°C/min to 900°C under a constant flow of air (50 ml/min) to obtain the char burning profile. The pyrolysis kinetics are assumed to follow an overall apparent first order reaction, and the Arrhenius parameters were evaluated as before [19].

In order to study the combustion behavior, single particles of the Nigerian woody biomass, were burned in a methane-air flame using a technique previously described. [33,34]. The experiments involved suspending cube-shaped fuel particles (2mm x 2mm x 2mm) on a

stainless steel needle in a Natural gas flame using a Meker type-burner. The temperature of the flame at the location of the particle was ~1200°C and the oxygen concentration was 10.8 ± 0.3 mol%. The particle was kept in a protective water-cooled sheath which was retracted to expose the fuel particle to the methane-air flame. A high speed video camera was used to record the images of the combustion at a speed of 125 frames/s.

3.0 Results and Discussion

3.1 The influence of torrefaction

Proximate analysis results are given in Table 2 together with the Higher Heating Value (HHV) and values for % Mass Yield (MY) and % Energy Yield (EY). Li et al. [21] have proposed that the torrefaction process can be evaluated by the 'degree of torrefaction', which is defined by them as the released volatiles divided by the initial volatile content of the raw material on dry-ash-free basis. These values are also given in Table 2. Effectively in energy terms there are equivalent to the loss in the EY values. There is quite a close correlation between these and the 'degree of torrefaction' except for the extreme values; exact agreement is not expected because there is preferential loss of molecular oxygen. In practice the degree of torrefaction is easier to use but the EY values give more exact information.

Moisture loss with increasing torrefaction temperature was found in the study of pine wood chips and logging wood chips torrefied at different temperatures of 250, 255, 270 and 300°C and at a residence time of 30 min [35]. The trend of decreasing volatile content is also observed, ranging from 57.5-80.9% and this is quite similar to that obtained by Ohliger et al. [36] from torrefaction of beechwood. Fixed carbon content increased with the longer residence time as the extent of pyrolysis increased, resulting in the preferential loss of oxygen and hydrogen over carbon; this can also be observed from the ultimate analyses shown in Table 2. The fixed carbon contents are in the range of 17.4-36.3% and are comparable to those obtained by Phanphanich et al. [35] for torrefied wood chips and logging residue.

The increase in carbon content results in higher HHV for the torrefied fuels, which range from 21.2 to 25.6 MJ/kg. Accordingly, most of the torrefied samples, like G270-30, G270-60, N270-30 and N270-60, have heating values which are comparable to those of subbituminous coals or high volatile bituminous coals. In general, *Terminalia* was found to have the lowest HHV values, both in raw or torrefied form. Nitrogen contents are discussed later. Sulphur contents were below 0.01%.

Typically, values of about 70% mass and 90% energy yields are often used as the benchmark to illustrate the energy densification benefit of the torrefaction process. The yields for different biomass vary, and largely depend on biomass compositions and reaction conditions [37]. The mass and energy yields obtained here are listed in Table 2. The mass yields ranged from 69.9% to 92.7%, while energy yield ranged from 77.2% to 93.3%, and both mass and energy yields decreased as the torrefaction condition increased. From the samples torrefied at 270°C for 30 min, PKE was the sample least affected by the torrefaction process. However, increasing the reaction time from 30 to 60 min resulted in optimum mass and energy yields, and the HHV produced under these conditions show they are more beneficial for this fuel than a higher process temperature. *Gmelina* had the lowest mass yield (73.9%), and *Nauclea* and *Terminalia* had the lowest energy yield (82.3 and 82.4 % respectively). Overall, G270-30 and P290-30 produced the lowest mass yield and energy yield (~ 69.9 and 77.2% respectively). In all cases increasing the reaction temperature resulted in lower mass and energy yields. These results are consistent with Chew and Doshi [37].

Figure 1 shows the overall mass balance resulting from torrefaction for the selected Nigerian fuels. The data has been corrected for moisture content and expressed in a dry basis of initial fuel mass. In this figure, "condensables" includes reaction water, and tar. Also gas yields are obtained by difference. GC analysis detected methane, carbon dioxide and carbon

monoxide. Depending on reaction conditions, gas yields are in the range 7-20% and condensable yields are in the range 9 to 18%.

3.2 Nitrogen Balance

The nitrogen content of untreated and torrefied biomass is of significance if they are used as fuels since the fuel-N is a major source of NOx. Of particular interest is whether torrefaction changes the fuel-N content. Few researchers have focused on nitrogen loss during torrefaction and there are some contradictory findings. The first published study was by Tumuluru [38]. In general there is marginal nitrogen loss upon torrefaction on a mass basis. When the severity of the process conditions were increased (typically to 350°C with a residence time of 120 min) there tends to be a greater loss.

In this work the variation in nitrogen content is given in Table 2 and given the accuracy in nitrogen content measurements (±0.5 wt%) it is seen that there is no clear trend. The ratios of nitrogen in the torrefied samples to the raw samples are given in the left hand column in Table 3 and most of the samples are similar except for the *Gmelina* samples which have the lowest nitrogen content. This may indicate a difference in chemical structures for samples with low nitrogen contents. The relationship between nitrogen and carbon release is shown in the next column in Table 3 and from their ratio and it is apparent that usually nitrogen follows carbon loss except for *Gmelina*. The last column in Table 3 shows the effect on an equivalent energy basis where again, within experimental error, all the samples are similar except for *Gmelina*. The similarity of results over a wide range indicating that the release of nitrogen can be fuel dependent, and the evidence suggests that it is dependent on there being a low fuel nitrogen content and the way it is bonded to the carbon matrix. *Terminalia* is also slightly different possibly due to the calcium oxalate content which decomposes on torrefaction..

3.3 Grindability and particle size distribution

The calculated HGI (or HGIequiv) values for the four coals are similar to the known HGI values, and the standard error is ≤ 3.0. Table 4 shows the HGIequiv values obtained for the biomass fuels. These were also classified in terms of hardness using a classification proposed by Tichánek [30] in which a coal with a HGI<40 is classified as very hard, 40-60 is said to be hard, 60-80 is medium hard, 80-100 is soft, 100-120 is very soft, and HGI values >120 are classified as extremely soft. As seen from Table 4, the results indicate that torrefied samples become easier to grind than raw samples. This was expected to occur due to the decomposition of hemicellulose during torrefaction process since hemicellulose acts as a binder [16, 35, 45]. However, it can also be observed that the fuels easiest to grind were T270-60 (HGIequiv 45), N270-30 (HGIequiv 51) and N270-60 (HGIequiv 56), and all of these fuels still fall under the category of hard. All other samples are classed as very hard, since their HGIequiv is below 40. The fuels studied here have higher grindability indices than the torrefied willow and miscanthus investigated by Bridgeman et al. [12], except for PKE that showed little improvement after torrefaction. These observations are consistent with the content of the inorganic species. The metal content in % wt ash for CaO and K_2O respectively as given in [9] are: Gmelina, 19.6/29.9; Terminalia, 41.7/8.4; Lophira, 41.0/8.2; Nauclea,9.3/32.0; PKE, 5.8/2.5. It is noted that PKE has 57.1 wt% of SiO_2 in ash, which is much higher than the woods where SiO_2 are all less than 10 wt %. This and the type of fibre impacts on the grindability of PKE after torrefaction.

The grindability behaviour of the samples after torrefaction is reflected in the particle size distribution after milling and these were plotted and compared to the results obtained for four standard reference coals,. The particle size distribution curves of raw and torrefied fuels are shown in Figures 2a-d for *Gmelina*, *Lophira*, *Terminalia* and *Nauclea*, respectively and the results for PKE are shown in Figure 3 (a). The low friability of the raw fuels is evident from

all these plots and in all cases it can be observed that torrefaction resulted in a higher proportion of finer particles. However, for fuels like *Gmelina, Lophira* and PKE, even the torrefied samples resulted in particle size distribution profiles with much less fines than those of the reference coals. For the fuels and torrefaction conditions studied here, only the torrefaction of *Nauclea* (N270-30 and N270-60) and *Terminalia* at the most severe conditions (T270-60) resulted in curves comparable to those of coals.

Generally, for all samples, *Nauclea* tends to be the easiest to grind, while PKE and Lophira seems to be the toughest. Hence, a relatively higher throughputs and lower mill power consumption is expected for torrefied *Nauclea* during milling than the other samples processed under similar torrefaction conditions.

3.4 Lignocellulose Analysis

The bio-chemical composition of the biomass was determined before and after torrefaction and the results are presented in Table 5; it is seen that the bio-chemical properties of the woods change depending on the severity of the torrefaction. The results in Table 5 show that during the torrefaction process at a temperature of 270°C, almost all the hemicellulose content of the fuels has reacted. The effect of increased residence time (to 60 min) was seen as the hemicellulose content in the fuels was completely decomposed, except in the case of *Nauclea,* which had 2.24% of hemicellulose content left. Torrefaction at 270°C for 30 minutes resulted in the decrease of cellulose: ~7.3% for *Lophira* and *Gmelina*, whilst further cellulose decomposition was experienced by PKE and Nauclea (~14-16%). However, in the case of *Terminalia* <2% of the cellulose was lost under the same conditions (Table 5). A further reduction in the cellulose content was observed when the fuels were torrefied at the same temperature for longer residence time of 60 minutes, as shown in Table 5. Upon torrefaction at this condition, the content of cellulose found in the fuels is 46.5, 45.2, 50.4, 28.7 and 41.4 (%) for *Lophira, Terminalia*, *Gmelina*, PKE and *Nauclea* respectively.

The results here are consistent with data for other biomass materials eg [17, 39] in that the lignin content increased upon torrefaction. The results from two analytical methods of assessing lignin in the fuels are also reported in Table 5. From this table it is seen that the lignin in the fuels (as assessed by both methods) concentrated upon torrefaction at the mild process condition, and its content increases further as the torrefaction conditions becomes more severe. The crude lignin content (measured by the ADL method) increases from 29.5% to 40.0, 28.6% to 4.4%, 22.9% to 32.0%, 21.6% to 24.8% and 33.0% to 44.1% when torrefied at 270°C for 30 min for *Lophira*, *Terminalia, Gmlina,* PKE and Nauclea respectively. Additionally, increasing the residence time from 30 to 60 minutes causes further increase in the lignin content of the fuels, as reported in Table 5. The results for the Klason lignin are significantly different from those obtained by the ADL method: the estimated concentrations of Klason lignin are much higher than by the ADL method – this is possibly because the ADL method for lignin determination underestimates lignin concentration due to loss of acid-soluble lignin in the acid detergent step of the procedure as discussed by Jung et al. [40]. Additionally, the increasing content of lignin observed upon torrefaction supports the conclusion of Shoulaifar et al. [39], who propose that the effect is likely due to two main reasons: (i) cellulose degradation products that can potentially result in acid-insoluble condensed and (ii) benzenoid aromatic groups, that is tars [41], which can increase the acid-insoluble material.

PY-GC-MS data was obtained for the four woods and PKE and the results are given in the Supplementary Data for the raw and torrefied samples. These add additional evidence for the above conclusions.

3.6 TGA Analysis

Thermogravimetric measurements were made of all the fuels and plots of the first derivative of mass loss curve with temperature (DTG) for the pyrolysis of the raw and torrefied samples are shown in Figures 4a-d for the woods and in Figure 3 (b) for PKE. The DTG pyrolysis curves show the main decomposition stages of pyrolysis characteristic of the fuels. The first stage of the curve is the moisture loss stage, which occurs between ≤110°C and is less evident in drier torrefied fuels. This stage is immediately followed by the devolatilization, which shows the greatest mass loss due to volatile release. In this instance, some of the curves revealed a shoulder on the pyrolysis peak (e.g. *Lophira* and *Terminalia*), or two partially resolved peaks for PKE (see Figure 3b). Both the unresolved peak at a lower temperature and the shoulder on the main peak are due to hemicellulose decomposition, but the main peak is predominantly due to the degradation of cellulose. The DTG curves of raw and torrefied *Terminalia* show additional peaks at higher temperatures that have been observed by Lasode et al. [10] for untreated and torrefied Nigerian *Terminalia ivorensis*, and by Fisher et al [18] from pure xylan. In the latter study the additional peaks can only be from the formation and carbonisation of higher molecular weight species such as biomass tars, for example, those derived from eugenol [41]. The last two peaks in the DTG pyrolysis curve for *Terminalia* however result from fuel ash, that is, from the decomposition of calcium oxalate in the fuel ash in this high calcium containing biomass (41.7wt% CaO in the ash).

Evidence for this assumption was confirmed by TGA pyrolysis of $CaC_2O_4.xH_2O$ and also of a small amount of CaC_2O_4 mixed with *Terminalia*. The DTG pyrolysis plots for *Terminalia*, $CaC_2O_4.xH_2O$, and a mixture of both *Terminalia* and $CaC_2O_4.xH_2O$ were plotted, as shown in Figure 5. It is evident from these plots that the last two weight loss steps at T>450°C on the DTG pyrolysis curve for *Terminalia* are due to the decomposition of $CaC_2O_4.xH_2O$ present in the fuel.

Table 6 shows the onset temperature (T_o) and temperature for the maximum rate of pyrolysis (T_{p1}) for the raw and torrefied fuels which were obtained from the DTG plots. It can be observed that the DTG peak pyrolysis temperatures for fuels torrefied at same temperature but different residence time have almost the same values. The pyrolysis peak temperature is often used as an indicator for fuel reactivity, where the fuels with the lowest T_{p1} value are considered the most reactive [42,43]. According to this, *Nauclea* and *Gmelina* (325°C) are ranked as the most reactive fuels, and torrefied PKE (357°C) is expected to be the least reactive of the fuels studied here. The potassium content in the fuels can influence its reactivity at devolatilisation and char burnout [20,44], and this is the case here: *Nauclea* and *Gmelina* have the highest potassium ash contents (32.0 and 29.9wt % K_2O) and PKE has the lowest (2.2wt%). Also from Table 6, it was observed that torrefaction lowers the reactivity of the fuels, and fuels that were subjected to a more critical torrefation conditions (by increasing the residence time) appeared less reactive.

The residue left at the end of pyrolysis is the char and ash content of the sample. This residue was cooled, and then underwent temperature programmed combustion. Table 6 also lists the char ignition temperatures (T_i) and the maximum peak temperature for combustion (T_{p2}) as obtained from the char burning profiles of the fuels studied (not shown). In contrast to the peak temperatures for pyrolysis, which appear almost unaffected by the longer reaction times, the peak temperatures for char combustion were shifted to higher temperatures when the torrefaction reaction time is increased from 30 to 60 min. The exceptions are *Gmelina* and PKE, which show no change in peak temperature upon torrefaction.

The reaction rate parameters for the pyrolysis of the fuels were derived using equation (4) for data at <10% conversion. The pre-exponential factors, A (1/s), activation energies, E (kJ/mol) are presented in Table 7. The data in this table shows that increasing the torrefaction temperature and/or residence time resulted in higher pre-exponential factors and activation

energies required for the pyrolysis reaction. This is because the overall reaction rate parameters derived from the TGA data now represents those for the decomposition of cellulose.

In order to establish a ranking of the reactivity of the samples, the kinetic parameters obtained were used to estimate the reactivity of the fuels at 300°C (k_{573}), which have also been listed in Table 7, for comparison purposes. As expected, the raw samples were found to be more reactive than their torrefied counterparts, and the reactivity follows the order *Nauclea* > *Gmelina* > G270-30 > G270-60 > N270-30 > *Terminalia* > *Lophira* > N270-60 > L270-30 > L270-60 > T270-30 > T270-60> PKE > P270-30> P270-60 > P290-30. The order of reactivity calculated at 300°C follows the same order of ranking obtained when comparing the peak pyrolysis temperature order. Both *Nauclea* and *Gmelina* resulted in very similar Ea values (77.8 and 78.8 kJ mol^{-1} respectively), which were the lowest activation energies observed and resulted in the fastest reactivities calculated. A possible reason for the low activation energy of *Gmelina* and *Nauclea* is the abundance of potassium in the fuel.

3.7 Single particle combustion as a measure of combustion reactivity.

The combustion of single particles provides information which is applicable to both pulverized fuel combustion but also to larger particles in fluidized bed combustion. The video images showed the combustion behaviour of the fuels. The following combustion stages were clearly identified from these images: ignition, volatile combustion, and char combustion permitting. estimation of their duration. In this instance only the raw fuels and the fuels torrefied at a process condition of 270°C for 60 min were studied in order to establish a clear distinction between their combustion properties. The fuel particle was taken to be ignited once flaming combustion was visible after exposure to the methane-air flame. This process is determined by the size of the particle or rather the Biot Number, Bi, the dimensionless ratio of surface convective heat transfer to internal heat conductivity (and determines whether the

heat conduction inside a particle is faster than that to the exterior of the particle from the flame). According to Hayhurst [45], a Bi value <0.1 will result in a more or less uniform temperature throughout the particle. In this instance, the Biot number for the untreated and treated fuels is different, consequently, the effect is observed in the heating-up process and the ignition delay of the fuels (untreated and torrefied), due to the differences in the thermal conductivity of the woods. The thermal conductivity of the torrefied fuels is higher since the thermal resistance of the wood is lowered by the torrefaction process.

The water content in the fuel particle is also important since it results in a delay in the ignition process and can lead to unstable fuel flames. Here ignition delay is obtained by the difference between the time at which the particle was exposed to the flame and the time at which the particle was ignited. A plot of the ignition delay against biomass particle dry mass is presented in Figure 6. From Figure 6, it can be observed that there are differences in the ignition delay of the raw and torrefied fuels. For the raw fuels, the effect of particle mass on the ignition delay of *Nauclea* and *Gmelina* is not as significant as in the case of *Terminalia* and *Lophira*. This is probably due to the facxt that *Nauclea* and *Gmelina* have relatively lower moisture contents when compared with *Lophira*. From Figure 6, it can be seen that the raw samples had longer ignition delay times than the torrefied samples, since the latter were drier than their raw counterparts. The ignition delay of *Nauclea*, *Lophira, Terminalia* and *Gmelina* ranged from 0.03 – 0.05s, 0.03 – 0.11s, 0.04 – 0.10s, and 0.04 – 0.06s respectively, with standard error ≤ ± 0.008s. There is a significant improvement in the ignition of the torrefied fuels, as the delay in ignition was reduced to about 0.02 - 0.03s (standard error ≤ ± 0.008s). It is important to mention that any differences in the ignition delay may have also occurred in part from the difficulty in reducing particles to exactly the same size and shape, and also, in part to the differences in moisture contents of individual particles. Moisture

contents were measured to be 4.2, 4.9, 5.2 and 12% for *Nauclea, Gmelina, Terminalia* and *Lophira* respectively, and less than 3% for the torrefied fuels.

Volatile combustion proceeds after ignition, where the particle devolatilises and volatile organic materials are released and combusted rapidly. The release of volatiles through the biomass pores prevents the ingress of external oxygen into the particle, i.e. the flow of oxygen into the particle is obstructed by the large gaseous outflow of volatiles from the surface of the particles. Thus, char combustion proceeds after devolatilisation, although in most cases here, an overlapping occurrence of volatile (flaming) combustion and char (glowing particle) combustion was observed whereby char combustion proceeded at the bottom of the particle while 'flame' combustion cotinued from the top of the particle.

Figure 7 shows the duration of volatile combustion plotted against original particle dry mass. The time taken for volatile combustion was measured as the difference between the time (or frame) at which the particle was ignited and the time at which the flame ends. From Figure 7, it can be seen that the raw fuels showed longer duration for flaming combustion when compared to torrefied fuels. Also the torrefied fuels appear to have similar durations for volatile combustion. The flame duration for Gmelina Terminalia, Lophira and Nauclea ranged from 2.02-3.74s, 2.38-3.53s, 3.22-4.21s, and 3.37-5.26s respectively (error $\leq \pm$ 0.008s). Whilst torrefied fuels: G270-60, T270-60, N270-60 and L270-60 resulted in flame combustion durations of 1.48-3.31s, 1.62-3.38s, 2.21-2.80s and 2.25-3.12s respectively (error $\leq \pm$ 0.008s). The difference in the duration of flame combustion could also possibly be due to the presence of catalytic metals in the fuels, the variations in the density of the woods, and slow release of volatile materials (reactivity and pore development upon torrefaction) during combustion.

At the end of devolatilisation, when the volatile flame ceases, and oxygen is able to reach the residual char particle, then heterogeneous char combustion begins. This process

continues until the char starts to shrink which happens more rapidly towards the end of the combustion reaction, and finally reduces to a small mass of ash. Video analysis constantly revealed a "shrinking sphere" model for char combustion (Zone II or III) where diffusion processes influence the combustion rate, and diffusion limitations became more crucial towards the end of char combustion. The duration of char combustion was assessed as the time it takes for the char to completely burn out, and this was estimated from the end of flame combustion (even though overlapping of these two processes could be observed) until nothing but ash remaining on the supporting needle (end of particle shrinkage). Figure 8 shows the plot of duration of char burnout versus original particle dry mass for the raw and torrefied fuels. From this figure, the char combustion step for raw *Lophira* and *Nauclea* particles showed different characteristics with longer char burnout stages, 9.74-19.15s and 21.64-39.52s respectively while the duration for char burnout of *Terminalia* and *Gmelina* ranged from 7.7-11.89s and 7.83-11.41s respectively (error ≤ ± 0.008s) and were comparable. It can also be seen that torrefied samples take longer to complete char burnout than the raw samples. The duration for char burn out for T270-60, G270-60, L270-60 and N270-60 is 17.74-45.02s, 10.66-23.88s, 39.94-47.27s and 34.43-54.60 respectively. The longer duration of the char combustion stage could result from the high char content (fixed carbon) of thermally pre-treated fuels. Moreover, diffusion rates, char porosity, the amount of catalytic metals present in the char, density of the wood, and elemental carbon content of the resultant char can also be contributing factors to the differences in char combustion rates. A relationship can be established between the maximum peak temperature for combustion (Table 5) and the duration of char burnout from the single particle combustion experiments. For example, N270-60 (T_{p2} 485°C) which was the least reactive from TGA also had the longest char burnout time (54.60 s).

It is clear that Nigerian woods and a major waste product (PKE) are sufficiently reactive as fuels to be used in pulverized combustors alone or blended with coal, although the woods are the preferred fuel because they can be milled more easily. Both could be used in fluidized bed combustor especially alone or blended with coal since larger fuel particles can be used. These could make a significant contribution to the local economy [3].

4.0 Conclusions

Four Nigerian woods, *Nauclea, Gmelina, Terminalia* and *Lophira,* and one residue, palm kernel expeller (PKE) have been evaluated for the effect of torrefaction on their combustion properties.

(1). After torrefaction, the samples had an improved HHV values. Many of the torrefied samples had heating values which are comparable to those of high volatile bituminous coals.

(2). The torrefaction process did not result in an improved fuel-nitrogen content on an energy basis. But only in one case, *Gmelina,* which has a low fuel-nitrogen content, there was an improvement.

(3), Torrefaction improved the grindability of all woods, but particularly T270-60, N270-30 and N270-60, all other samples were "very hard", although they showed improved milling behaviour compared to their raw counterparts. Torrefied PKE, however, showed little improvement even when a more severe torrefaction condition was applied due to the high SiO_2 content and type of fibre.

(3). TGA analysis showed that torrefied fuels are less reactive during pyrolysis than their raw counterparts, and the more severe the torrefaction conditions, the less reactive the fuels became.

(4). The combustion behaviour of selected raw and torrefied fuels was examined in a methane air flame using a high speed camera. The observations showed that torrefaction changed the combustion properties of biomass resulting in shorter ignition delay, shorter duration of volatile combustion and longer duration of char burn out. The torrefied fuels studied would be ideal in applications to pulverized power stations as well as in fluidized combustors.

Acknowledgments.

The authors are grateful to the UK Energy Programme (Grant EP/H048839/1) for partial financial support. The Energy Programme is a Research Councils UK cross Council initiative led by EPSRC and contributed to by ESRC, NERC, BBSRC and STFC. F.S. Akinrinola is also thankful to the Niger Delta Development Commission (NDDC) Overseas Scholarship Scheme, for partly funding his PhD studies. Special thanks to Quintas Renewable Energy Solutions Limited for supplying the Nigerian fuels.

References

[1] IPCC, 2018: Global Warming of 1.5°C. An IPCC Special Report on the impacts of global warming of 1.5°C above pre-industrial levels and related global greenhouse gas emission pathways, in the context of strengthening the global response to the threat of climate change, sustainable development, and efforts to eradicate poverty, V. Masson-Delmotte, P. Zhai, H.-O. Pörtner, D. Roberts, J. Skea, P.R. Shukla, et. al., (eds.)]. October 2018.

[2] Many coal projects in Africa make neither environmental nor financial sense. Anon, The Economist, July 27 (2019).

[3] F.O. Olanrewaju, G.E. Andrews, H. Li, H N. Phylaktou, Bioenergy potential in Nigeria, Chemical Engineering Transactions, 74 (2019) 61-66.

[4] U. B. Akuru, I. E. Onukwube, O. I. Okoro, E. S. Obe, Towards 100% renewable energy in Nigeria, Renewable and Sustainable Energy Reviews, 71 (2016) 943-953.

http://dx.doi.org/10.1016/j.rser.2016.12.123.
[5] Y.S. Mohammed, M.W. Mustafa, N. Bashir, M.A. Ugundola, U. Umar, Sustainable potential of bioenergy for distributed power generation development in Nigeria, Renewable and Sustainable Energy Reviews, 34 (2014) 361-370.
[6] M. Kopczyński, J.A. Lasek, A. Iiuk. J. Zuwała, The co-combustion of hard coal with raw and torrefied biomasses (willow (Salix viminalis), olive oil residue and waste wood from furniture manufacturing), Energy 140 (2017) 1316-3125.
[7] A. Williams, M. Pourkashanian, J.M. Jones, Combustion of pulverised coal and biomass. Progress in Energy and Combustion Science 27(6) (2001) 587-610.
2010.
[8] J. Li, A. Brzdekiewicz, W. Yang, W. Blasiak, Co-firing based on biomass torrefaction in a pulverized coal boiler with aim of 100% fuel switching, Applied Energy 99 (2012) 344-354.
[9] F.S. Akinrinola, L.I. Darvell, J.M. Jones, A. Williams, J.A. Fuwape, Characterization of selected Nigerian biomass for combustion and pyrolysis applications, Energy Fuels, 28 (2014) 3821-3832.
[10] O.A. Lasode, A. O. Balogun, A. G. McDonald, Torrefaction of some Nigerian lignocellulosic resources and decomposition kinetics, Journal of Analytical and Applied Pyrolysis 109 (2014) 47–55.
[11] B. Arias, C. Pevida, J. Fermoso, M.G. Plaza, F. Rubiera, J.J. Pis, Influence of torrefaction on the grindability and reactivity of woody biomass. Fuel Processing Technology, 89 (2008) 169-175.
[12] T.G. Bridgeman, J.M. Jones, A. Williams, D.J. Waldron, An investigation of the grindability of two torrefied energy crops. Fuel 89(12) (2010) 3911-3918.
[13] R. Pentananunt, A.N.M. Mizanur Rahman, S.C. Bhattacharya, Upgrading of biomass by means of torrefaction. Energy 15(12) (1990) 1175-1179.
[14] P.C.A. Bergman, J.H.A. Kiel, Torrefaction for biomass upgrading, 14th European Biomass Conference & Exhibition, Paris, France, 17-21 October 2005
[15] M.J.C. Van der Stelt, H. Gerhauser, J.H.A. Kiel, K.J. Ptasinski, Biomass upgrading by torrefaction for the production of biofuels: A review. Biomass and Bioenergy, 35(9) (2011) 3748-3762.
[16] R H.H. Ibrahim, L. I. Darvell, J. M. Jones, A. Williams, Physicochemical characterisation of torrefied biomass. Journal of Analytical and Applied Pyrolysis, 103 (2013) 21-30.

[17] A. Anca-Couce A. Reaction mechanisms and multi-scale modelling of lignocelluosic biomass pyrolysis. Prog. Energy Combust. Sci. 2016; 53:41 – 79.
[18] T. Fisher, M. Hajaligol, B Waymack, D. Kellogg, Pyrolysis behavior and kinetics of biomass derived materials, Journal of Analytical and Applied Pyrolysis 62 (2002) 331–349.
[19] A. Saddawi, J. M. Jones, A. Williams, M. A. Wojtowicz, Kinetics of the thermal decomposition of biomass, Energy Fuels 24 (2010) 1274–1282.
[20] A. Saddawi, J.M. Jones, A. Williams. Influence of alkali metals on the kinetics of the thermal decomposition of biomass, Fuel Processing Technology, 104 (2012) 189-197.
[21] J. Li, G. Bonvicini, L. Tognotti, W. Yang, W. Blasiak, High-temperature rapid devolatilization of biomasses with varying degrees of torrefaction Fuel 122 (2014) 261–269
[22] H. Tolvanen, T. Keipi, R. Raiko, A study on raw, torrefied, and steam-exploded wood: Fine grinding, drop-tube reactor combustion tests in N_2/O_2 and CO_2/O_2 atmospheres, particle geometry analysis, and numerical kinetics modeling, Fuel 176 (2016) 153–164.
[23] J.M. Jones, T.G. Bridgeman, L.I. Darvell, B. Gudka, A. Saddawi, A. Williams, Combustion properties of torrefied willow compared with bituminous coals, Fuel Processing Technology, 101 (2012) 1-9.
[24] J. Li, G. Bonvicini, E. Biagini, W. Yang, L. Tognotti, Characterization of high-temperature rapid char oxidation of raw and torrefied biomass fuels, Fuel 143 (2015) 492–498.
[25] P. McNamee, L.I. Darvell, J.M. Jones, A. Williams, The combustion characteristics of high-heating-rate chars from untreated and torrefied biomass fuels, Biomass and Bioenergy 82 (2015) 63-72.
[26] J. Li, E. Biagini, W. Yang, L. Tognotti, W. Blasiak, Flame characteristics of pulverized torrefied-biomass combusted with high-temperature air, Combustion and Flame 160 (2013) 2585–2594.
[27] J.M. Jones, L. Ma, M. Pourkashanian, A. Williams, CFD modelling of the combustion of milled torrefied wood, Journal of the Energy Institute 84 (2011) 102-104.
[28] T.G. Bridgeman, J.M. Jones, I. Shield, P.T. Williams, Torrefaction of reed canary grass, wheat straw and willow to enhance solid fuel qualities and combustion properties, Fuel 87(6) (2008) 844-856.
[29] A. Friedl, E. Padouvas, H. Rotter, K. Varmuza, Prediction of heating values of biomass fuel from elemental composition, Analytica Chimica Acta. 544(1-2) (2005) 191-198.
[30] F. Tichánek, Contribution to determination of coal grindability using Hardgrove Method. GeoScience Engineering GSE, 54(1) (2008) 27-32.

[31] P.J. Van Soest, The use of detergents in the analysis of fibrous feeds: II. A rapid method for the determination of fibre and lignin, Journal of the Association of Official Agricultural Chemists 46 (1963) 829-835.

[32] B. Gudka, L.I. Darvell, J.M. Jones, A. Williams, P.J. Kilgallon, N.J. Simms, R. Laryea-Goldsmith, Fuel characteristics of wheat-based Dried Distillers Grains and Solubles (DDGS) for thermal conversion in power plants, Fuel Processing Technology 94(1) (2012) 123-130.

[33] J.M. Jones, L.I. Darvell, T.G. Bridgeman, M. Pourkashanian, A. Williams, An investigation of the thermal and catalytic behaviour of potassium in biomass combustion, Proceedings of the Combustion Institute, 31 (2007) 1955-1963.

[34] P.E. Mason, L.I. Darvell, J.M. Jones, M. Pourkashanian, A. Williams, Single particle flame-combustion studies on solid biomass fuels, Fuel 151 (2015) 21–30.

[35]. Phanphanich, M. and S. Mani, Impact of torrefaction on the grindability and fuel characteristics of forest biomass. Bioresource Technology, 2011. 102(2): p. 1246-1253.

[36]. Ohliger, A., M. Förster, and R. Kneer, Torrefaction of beechwood: A parametric study including heat of reaction and grindability. Fuel, 2013. 104(0): p. 607-613.

[37] Chew, J.J. and V. Doshi, Recent advances in biomass pretreatment – Torrefaction fundamentals and technology. Renewable and Sustainable Energy Reviews, 2011. 15(8): p. 4212-4222.

[38] J.S.Tumuluru, Effect of deep drying and torrefaction temperature on proximate, ultimate composition, and heating value of 2-mm Lodgepole Pine (*Pinus contorta*) grind, Bioengineering 3(2) (2016) 16: 1-18.

[39] T. K. Shoulaifar, N. DeMartini, S. Willför, A. Pranovich, A. I. Smeds, T. A. P. Virtanen, S-L. Maunu, F. Verhoeff , J. H. A. Kiel, M. Hupa, Impact of torrefaction on the chemical structure of birch wood, Energy Fuels 28 (2014) 3863−3872.

[40] H-J G. Jung, V.H. Varel, P.J. Weimer, J. Ralph, Accuracy of Klason Lignin and Acid Detergent Lignin methods as assessed by bomb calorimetry, Journal of Agricultural and Food Chemistry 47(5) 1999. 2005-200

[41] E.B. Ledesma, J.N. Hoang, Q. Nguyen, V. Hernandez, M.P. Nguyen, S. Batamo, C.K. Fortune, Unimolecular decomposition pathway for the vapor-phase cracking of eugenol, A biomass tar compound, Energy Fuels 27, (2013) 6839−6846.

[42] L.I. Darvell, J.M. Jones, B. Gudka, X.C. Baxter, A. Saddawi, A. Williams, A. Malmgren Combustion properties of some power station biomass fuels. Fuel, 2010. 89(10): p. 2881-2890.

[43] A. Saddawi, J.M. Jones, A. Williams, C. Le Coeur, Commodity fuels from biomass through pretreatment and torrefaction: Effects of mineral content on torrefied fuel characteristics and quality. Energy Fuels 26 (2012) 6466−6474.
[44] P.E. Mason, L.I. Darvell, J.M. Jones, A. Williams, Observations on the release of gas-phase potassium during the combustion of single particles of biomass, Fuel 182 (2016) 110–117.
[45] A.N. Hayhurst, The kinetics of the pyrolysis or devolatilisation of sewage sludge and other solid fuels, Combustion and Flame 160 (2013) 138–144.

Tables

Table 1. Sample designation, material and torrefaction conditions

Sample designation	Material and torrefaction conditions
Gmelina	Raw *Gmelina arborea* before torrefaction
G270-30	*Gmelina arborea* torrefied at 270°C for 30 minutes
G270-60	*Gmelina arborea* torrefied at 270°C for 60 minutes
Terminalia	Raw *Terminalia superba* before torrefaction
T270-30	*Terminalia superba* torrefied at 270°C for 30 minutes
T270-60	*Terminalia superba* torrefied at 270°C for 60 minutes
Lophira	Raw *Lophira alata* before torrefaction
L270-30	*Lophira alata* torrefied at 270°C for 30 minutes
L270-60	*Lophira alata* torrefied at 270°C for 60 minutes
Nauclea	Raw *Nauclea diderrichii* before torrefaction
N270-30	*Nauclea diderrichii* torrefied at 270°C for 30 minutes
N270-60	*Nauclea diderrichii* torrefied at 270°C for 60 minutes
PKE	Raw *Palm Kernel Expeller* before torrefaction
P270-30	*Palm Kernel Expeller* torrefied at 270°C for 30 minutes
P270-60	*Palm Kernel Expeller* torrefied at 270°C for 60 minutes
P290-30	*Palm Kernel Expeller* torrefied at 290°C for 30 minutes

Table 2. Proximate analysis (%), ultimate analysis (wt% daf), mass yield (MY), energy yield (EY) and HHV (db) for the raw biomass (given in bold) and the pyrolysed products.

Samples	MC (ar)	VM (db)	Ash (db)	FC[a] (db)	C (daf)	H (daf)	N (daf)	MY (%)	EY (%)	Degree of Torrefaction,%	HHV (MJ/kg)
Gmelina	4.9	80.9	1.0	18.1	51.9	6.3	0.16	100.0	100.0	0	20.8
G270-30	2.4	73.7	1.7	24.6	58.1	6.1	0.15	73.9	83.3	8.8	22.7
G270-60	2.1	69.8	1.8	28.5	58.6	5.7	0.14	69.9	78.8	13.7	23.1
Terminalia	5.2	80.2	2.2	17.4	50.1	5.9	0.33	100.0	100.0	0	19.4
T270-30	1.5	72.9	4.4	22.8	56.2	5.7	0.36	75.0	82.4	9.1	21.0
T270-60	1.5	68.3	6.3	25.4	58.7	5.3	0.50	71.9	80.2	14.8	215
Lophira	12.0	78.1	1.6	20.3	52.7	6.6	0.28	100.0	100.0	0	21.1
L270-30	2.6	70.8	2.0	27.2	57.5	5.6	0.27	81.1	87.0	9.3	22.5
L270-60	2.6	67.6	2.2	30.2	58.2	5.8	0.28	77.4	84.5	13.4	23.0
Nauclea	4.2	80.6	0.7	18.8	53.5	6.3	0.64	100.0	100.0	0	22.9
N270-30	2.5	66.0	1.0	33.0	58.1	5.7	0.70	75.9	82.3	18.1	23.4
N270-60	1.6	62.3	1.4	36.3	61.4	5.6	0.70	71.0	81.6	22.5	24.5
PKE	9.6	76.1	2.9	21.0	55.2	6.4	0.45	100	100	0	21.0
P270-30	3.5	70.4	5.0	24.6	58.0	5.4	0.50	92.7	93.3	7.4	21.5
P270-60	2.8	57.5	7.9	34.6	68.7	5.8	0.58	71.9	85.2	24.4	25.5
P290-30	3.4	65.7	5.2	29.1	60.4	5.2	0.55	74.4	77.2	13.6	22.6

ar, as received; db, dry basis; daf, dry ash free; HHV,Higher Heating Value; MC, moisture content; VM, volatile matter; FC, fixed carbon; MY, mass yield; EY, energy yield. The accuracy of these analyses is ±0.5 wt%

Table 3. Ratios of: nitrogen content before and after torrefaction (wt%, as received); atomic N to atomic C before and after torrefaction, and N on a kg/GJ) basis before and after torrefaction

Sample	$\{N_{Torr}\}$ / $N_{.Raw}$	$\{N/C_{(Torr)}\}$ / $\{N/C_{(Raw)}\}$	$\{N_{(Torr)\ kg/GJ}\}$/ $\{N_{(Raw)\ kg/GJ}\}$
G270-30	0.9	0.8	0.8
G270-60	0.9	0.7	0.8
T270-30	1.1	0.9	0.9
T270-60	1.3	1.1	1.2
L270-30	1.1	0.9	0.9
L270-60	1.1	0.9	0.9
N270-30	1.2	1.0	1.0
N270-60	1.2	1.0	1.0
P270-30	1.1	1.0	1.0
P270-60	1.3	1.1	1.0
P290-30	1.2	1.1	1.1

The accuracy of these ratios is ±10.0 wt%

Table 4. HGI_{equiv} of samples and hardness classification [30]

Sample	m%	HGI_{equiv}	HGI Interpretation
Raw *Gmelina*	0.4	0	Very hard
G270-30	1.7	14	Very hard
G270-60	3.2	23	Very hard
Raw *Terminalia*	0.5	0	Very hard
T270-30	2.0	16	Very hard
T270-60	7.0	45	Hard
Raw *Lophira*	0.7	0	Very hard
L270-30	1.7	15	Very hard
L270-60	2.0	16	Very hard
Raw *Nauclea*	1.0	0	Very hard
N270-30	8.0	51	Hard
N270-60	9.0	56	Hard
PKE	0	0	Very hard
P270-30	0.6	8	Very hard
P270-60	1.2	12	Very hard
P290-30	0.9	10	Very hard

Table 5. Lignocellulose component of the fuels and the corresponding estimated loss upon torrefaction (as received basis).

Fuel Sample	Cellulose wt %	Hemicellulose wt %	Lignin wt %	Klason Lignin wt %	Estimated loss upon torrefaction		
					Cellulose wt %	Hemicellulose wt %	Lignin wt %
Lophira	**52.76**	**7.72**	**29.49**	**34.68**	**0.00**	**0.00**	**0.00**
L270-30	48.89	0	40.97	48.08	33.84	100	0.80
L270-30	46.48	0	43.09	52.71	40.68	100	1.61
Terminalia	**46.89**	**10.47**	**28.62**	**30.4**	**0**	**0**	**0**
T270-30	46.02	0.05	41.38	44.28	33.07	99.67	1.41
T270-60	45.17	0	41.49	53.99	35.37	100	2,74
Gmelina	**56.1**	**9.93**	**22.93**	**33.13**	**0**	**0**	**0**
G270-30	52.04	2.04	32.02	44.87	34.81	85.56	1.86
G270-60	50.36	0	33.28	52.33	40.25	100	3.40
PKE	**39.05**	**11.01**	**21.62**	**43.23**	**0**	**0**	**0**
P270-30	33.62	5.99	24.77	55.44	33.82	58.18	11.93
P270-60	28.65	0	29.05	87.8	52.01	100	12.10
P290-30	32.83	2.15	28.08	64.29	43.09	86.78	12.08
Nauclea	**50.01**	**7.03**	**33.03**	**38.75**	**0**	**0**	**0**
N270-30	42.01	4.02	44.12	60.58	38.91	58.41	2.86
N270-60	41.37	2.24	46.44	62.65	43.72	78.32	4.34

Table 6. Characteristics temperature for the pyrolysis and combustion of the raw and torrefied samples

Sample	Pyrolysis onset temp (^{o}C) T_o	Pyrolysis Max. peak (^{o}C) T_{p1}	Combustion ignition Temp (^{o}C) T_i	Combustion Max. peak (^{o}C) T_{p2}
Gmelina	247	325	341	398
G270-30	273	328	345	401
G270-60	274	329	348	401
Terminalia	261	343	345	403
T270-30	290	348	352	411
T270-60	296	348	362	430
Lopira	264	345	391	425
L270-30	290	346	391	431
L270-60	292	346	393	446
Nauclea	252	325	360	428
N270-30	275	331	390	451
N270-60	292	345	409	485
PKE	251	352	390	485
P270-30	272	357	390	489
P270-60	292	357	390	489
P290-30	296	357	416	485

Table7. First-order kinetic parameters for the pyrolysis of the torrefied fuels

Sample	ln (A) (1/s)	Ea (kJ/mol)	Correlation co-efficient, R^2	Reactivity (1/s) at 573K, (K_{573})
Gmelina	10	78.8	0.9947	0.00150
G270-30	17.3	114	0.9956	0.00144
G270-60	20	128	0.9951	0.00108
Terminalia	15.6	110	0.9982	0.00052
T270-30	19.5	131	0.999	0.00035
T270-60	24.5	155	0.9961	0.00033
Lophira	15.9	112	0.9801	0.00051
L270-30	23.3	148	0.9985	0.00045
L270-60	24.9	156	0.9927	0.00042
Nauclea	9.87	77.8	0.9953	0.00157
N270-30	18.2	120	0.9959	0.00092
N270-60	16.7	116	0.9953	0.0005
PKE	14.5	108	0.9985	0.00033
P270-30	19.8	133	0.9797	0.00033
P270-60	23.2	149	0.9948	0.00031
P290-30	19.7	133	0.9848	0.00028

Figure legends

Figure 1. Overall mass balance resulting ftom torrefaction for the selected fuels.

Figure 2. Particle size distribution curves for raw and torrefied (a) *Gmelina*, (b) *Terminalia,* (c*) Lophira*, (d) *Nauclea* and (e) PKE, all plotted alongside the particle size distribution of four standard reference coals of HGI 26, 49, 69 and 94.

Figure 3. (a) Particle size distribution curves for raw and torrefied PKE plotted alongside the particle size distribution of four standard reference coals of HGI 26, 49, 69 and 94, and (b) DTG pyrolysis profile of raw and torrefied PKE.

Figure 4. DTG pyrolysis profile of raw and torrefied: (a) *Gmelina*, (b) *Terminalia,* (c) *Lophira*, (d) *Nauclea* and (e) PKE

Figure 5. DTG pyrolysis profile of raw Terminalia, $CaC_2O_4.xH_2O$ and $CaC_2O_4.xH_2O$ *Terminalia*

Figure 6. Plot of the ignition delay against particle mass (dry) for raw and torrefied fuels.

Figure 7. Plot of flame combustion duration against particle mass (dry) for raw and torrefied fuels.

Figure 8. Plot of the char burnout duration against original dry particle mass for raw and torrefied fuels.

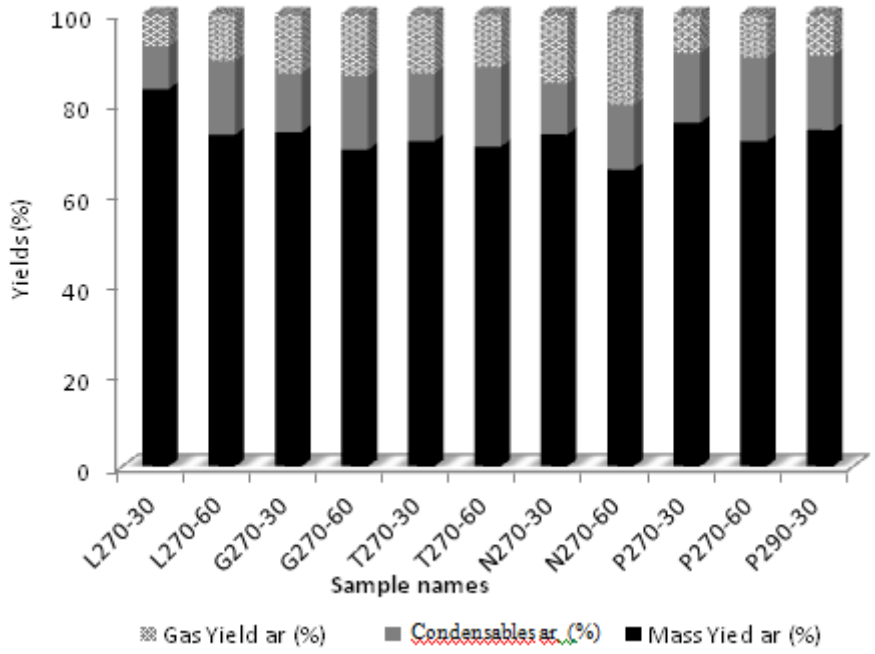

Figure 1. Overall mass balance resulting from torrefaction for the fuels studied.

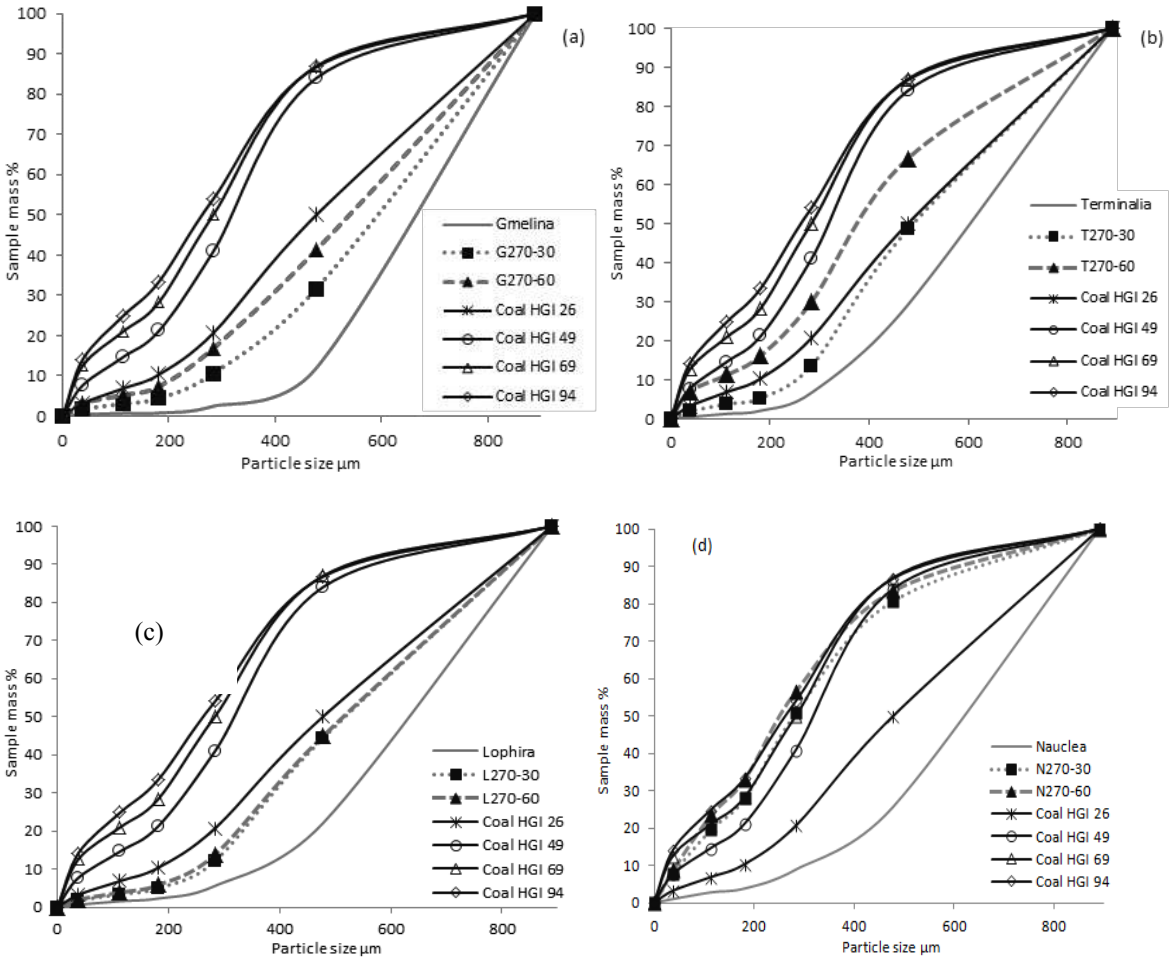

Figure 2. Particle size distribution curves for raw and torrefied (a) *Gmelina,* (b) *Terminalia,* (c*) Lophira*, (d) *Nauclea* plotted alongside the particle size distribution of four standard reference coals of known HGI.

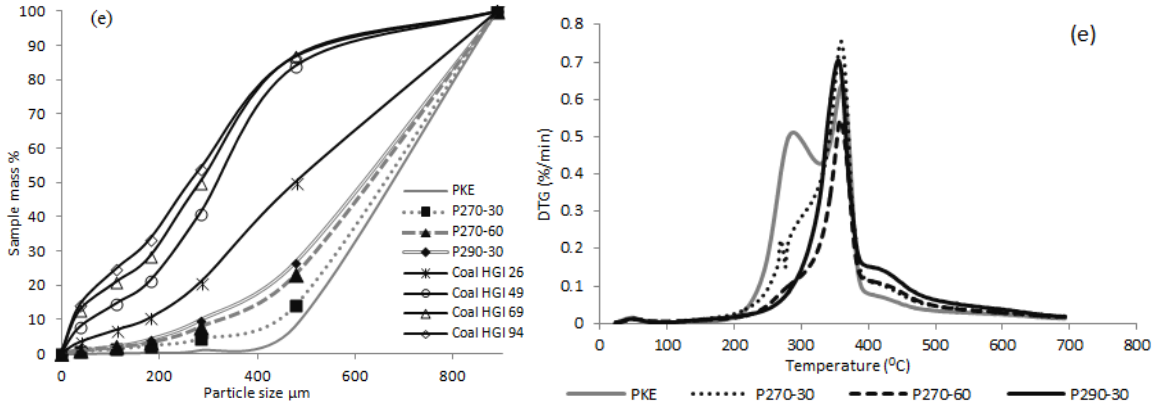

Figure 3. PKE: (a) Particle size distribution curves for raw and torrefied PKE, all plotted alongside the particle size distribution of the standard HGI reference coals, and (b) DTG pyrolysis profile of raw and torrefied PKE

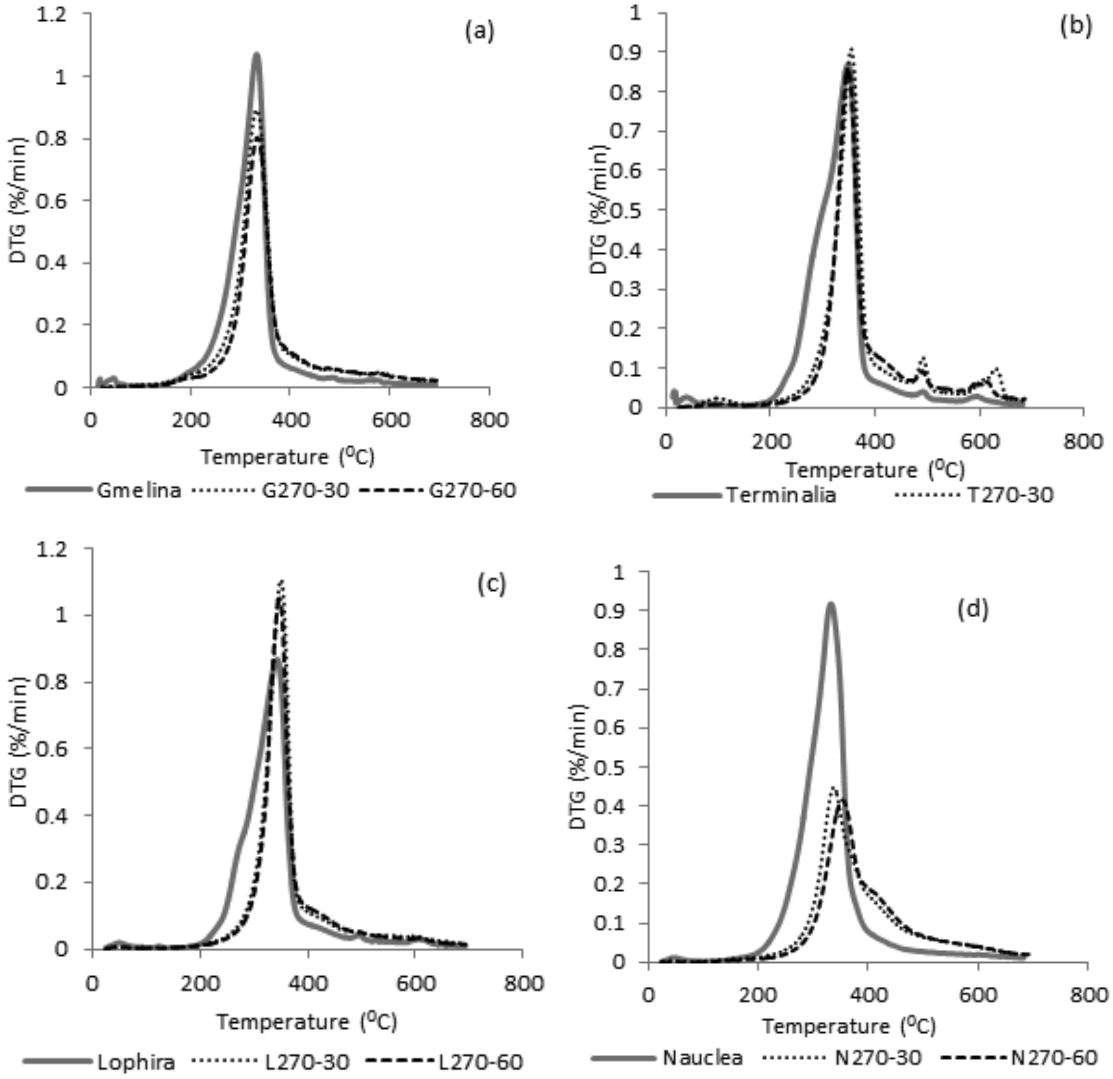

Figure 4. DTG pyrolysis profile of raw and torrefied: (a) *Gmelina*, (b) *Terminalia,* (c) *Lophira*, and (d) *Nauclea*

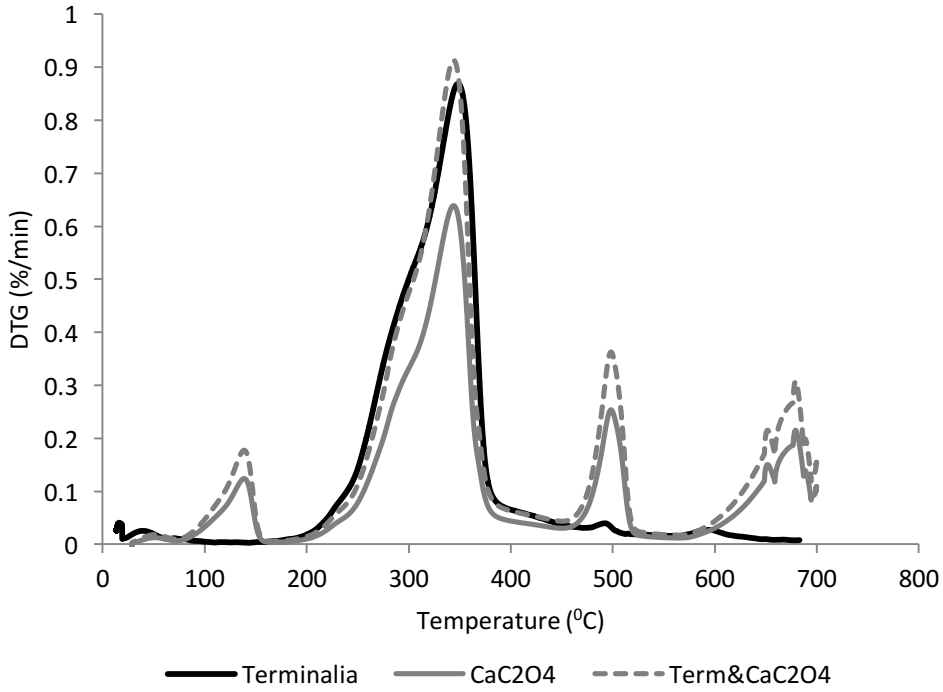

Figure 5. DTG pyrolysis profile of raw *Terminalia*, $CaC_2O_{4x}H_2O$, & $CaC_2O_{4x}H_2O$ + *Terminalia*.

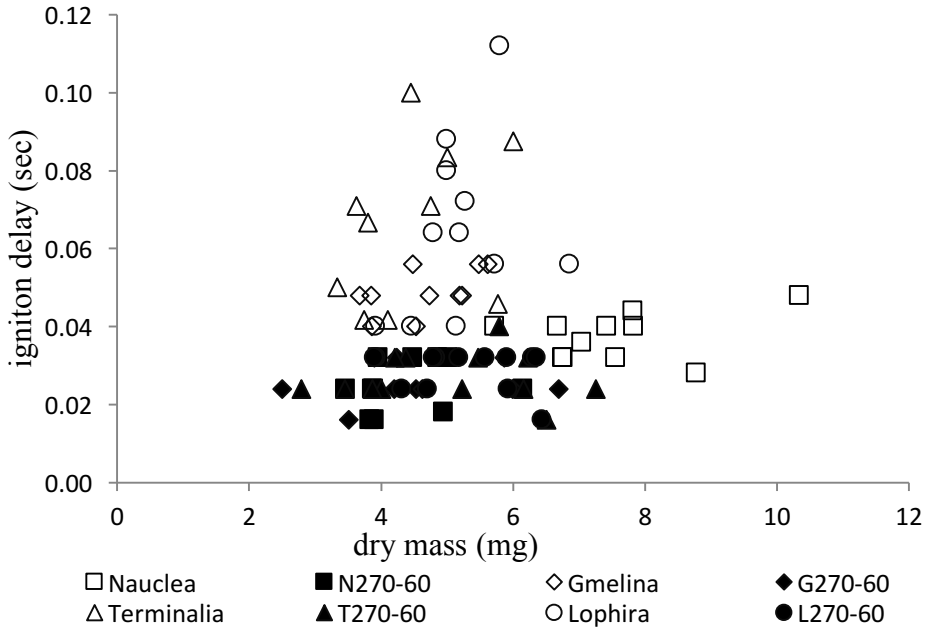

Figure 6. Plot of the ignition delay against particle mass (dry) for raw and torrefied fuels.

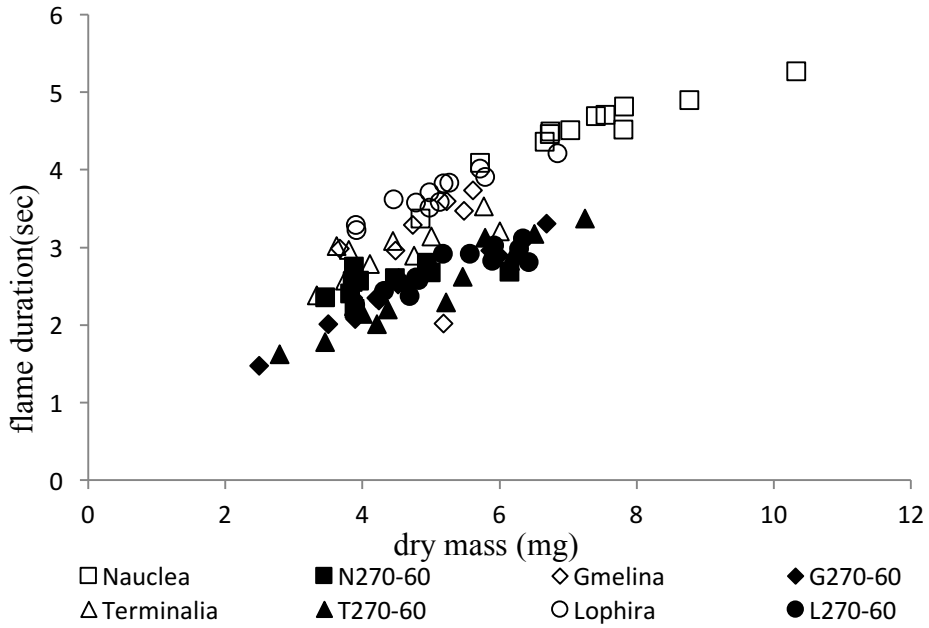

Figure 7. Plot of flame combustion duration against particle mass (dry) for raw and torrefied fuels.

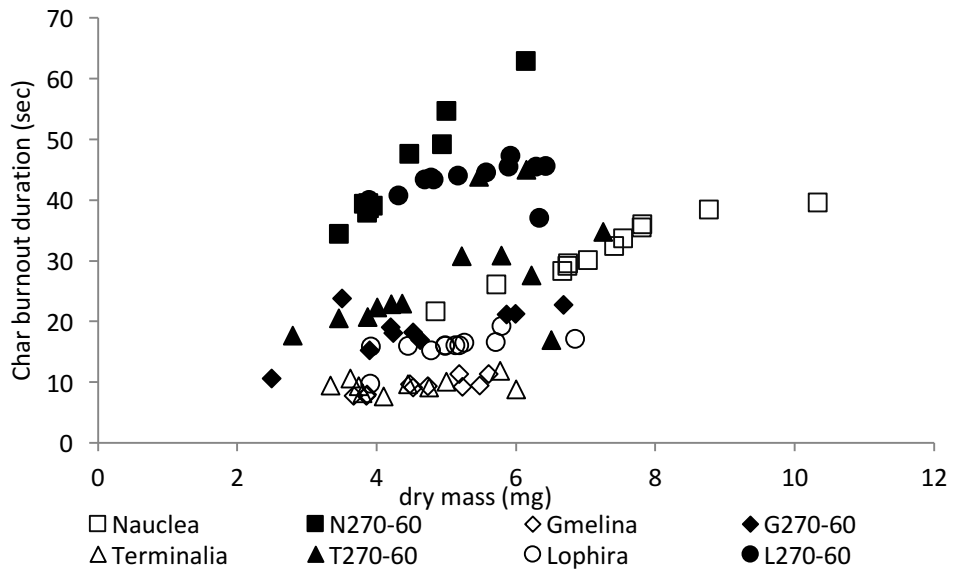

Figure 8. Plot of the char burnout duration against original dry particle mass for raw and torrefied fuels.

Supplementary Data

1. Py-GC-MS Measurements

   The Py-GC-MS analyses were carried out on the samples using a CDS 1000 Pyroprobe attached to a HP 5890 series II Gas Chromatograph which was fitted with a Rtx 1701 60 m capillary column (0.32 id and 0.25μm film thickness) and using He gas as a carrier. The oven was held at a temperature of 70°C for 120 s and then programmed at 20/°C min to a final temperature of 250°C, and held for 15 min. Approximately 2-3 mg of sample were held between plugs of quartz wool in a 2mm diameter, 20 mm long silica tube. The sample was then pyrolysed at a maximum temperature of 600°C with a nominal ramp rate of 20°C/min and a final dwell time of 20 s. Products were identified using mass spectral detection using the NIST 05A MS library.

   Further details of the methods used are given in 'Torrefaction and Combustion Properties of some Nigerian Biomass' by F. S. Akinrinola, PhD thesis, University of Leeds. December, 2014.

   The following Figures give the decomposition products from Py-GC-MS analysis of raw and torrefied *Gmelina, Terminalia, Lophira, Nauclea* and PKE.

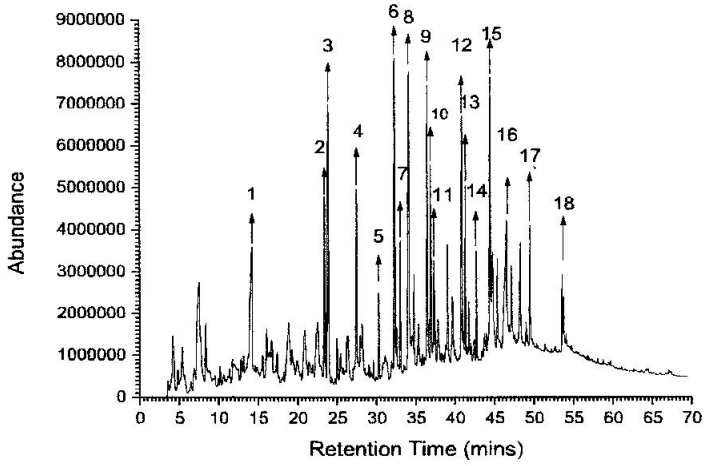

1

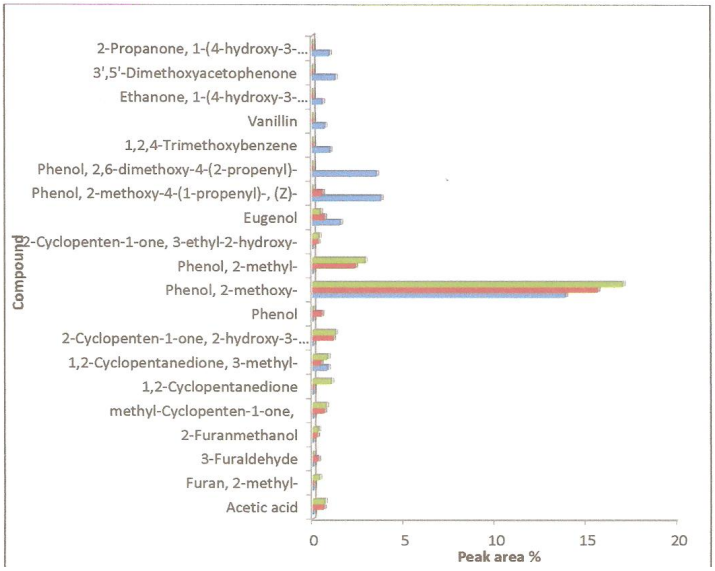

Figure S ! (b). Decomposition products from Py-GC-MS analysis of raw and torrefied *Gmelina.*

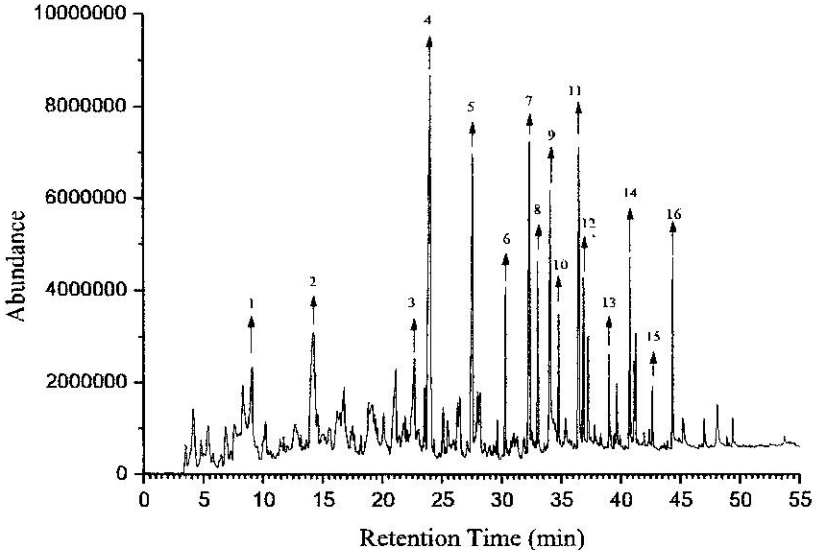

Figure S2 (a). Py GC-MS chromatogram of *Terminalia* showing assigned peaks.

The main peaks are assigned as follows: 1:1,3-pentadiene, 2: cyclohexanol, 1-methyl-4(1-methylethenyl)-, acetate; 3: 1,2-cyclopentanedione, 3-methyl; 4: phenol; 5: 2methoxyphenol; 6: 2-methoxy-4-methylphenol; 7: 4-ethyl-2-methoxyphenol; 8: 2methoxy-4-vinylphenol; 9: eugenol; 10: 2,6-dimethoxyphenol; 11: 2-methoxy-4-(1propenyl)-phenol; 12: 1,2,4-trimethoxybenzene; 13: vanillin; 14: ethanone, 1-(4hydroxy-3-methoxyphenyl); 15: 3',5'-dimethoxyacetophenone; 16: 2,6-dimethoxy-4-(2propenyl)phenol.

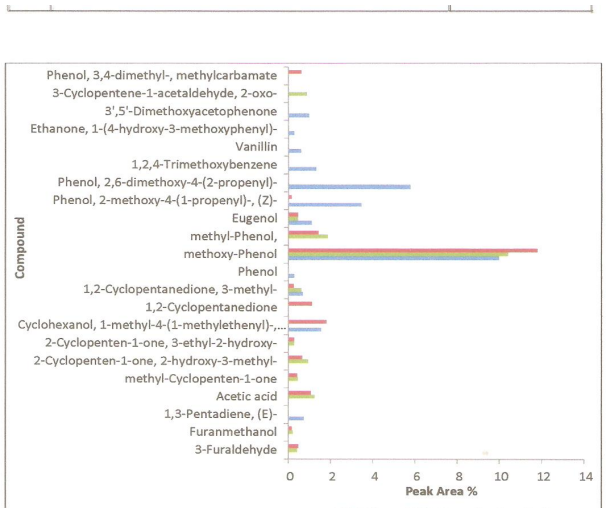

Figure S2 (b). Decomposition products from Py-GC-MS analysis of raw and torrefied *Terminalia*.

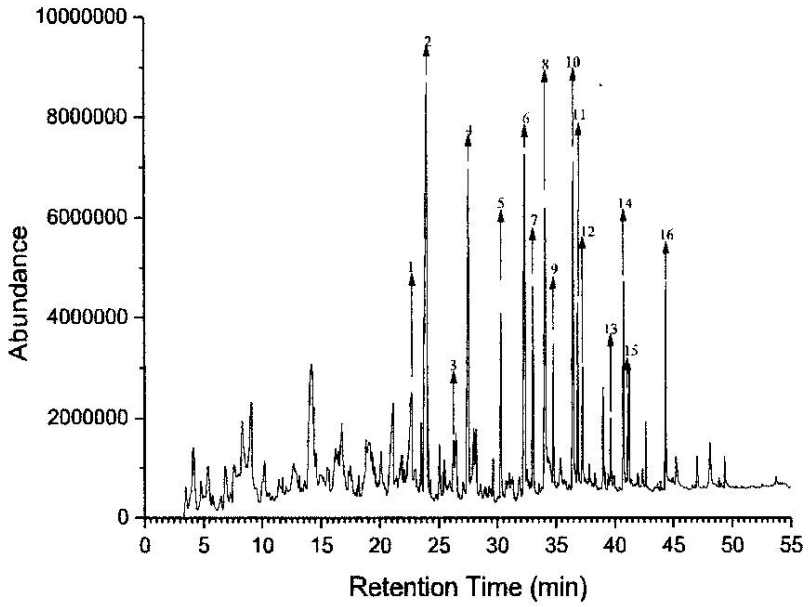

Figure S3 (a). Py GC-MS chromatogram of *Lophira* showing assigned peaks.

The main peaks are assigned as follows: 1: 1,2-Cyclopentanedione, 3-methyl; 2: 2methoxyphenol; 3: 2-methoxy-3-methylphenol; 4: 2-methoxy-4-methylphenol; 5: 4ethyl-2-methoxyphenol; 6: 2-Methoxy-4-vinylphenol; 7: eugenol; 8: 2,6dimethoxyphenol; 9: 2-methoxy-4-(1-propenyl)phenol; 10: 1,2,4-trimethoxybenzene; 11: vanillin; 12: ethanone, 1-(4-hydroxy-3-methoxyphenyl)-; 13: 3',5'dimethoxyacetophenone; 14: 2-propanone, 1-(4-hydroxy-3-methoxyphenyl)-; 15: 2,6dimethoxy-4-(2-propenyl)phenol; 16: 2,4-hexadienedioic acid, 3,4-diethyl-dimethyl ester

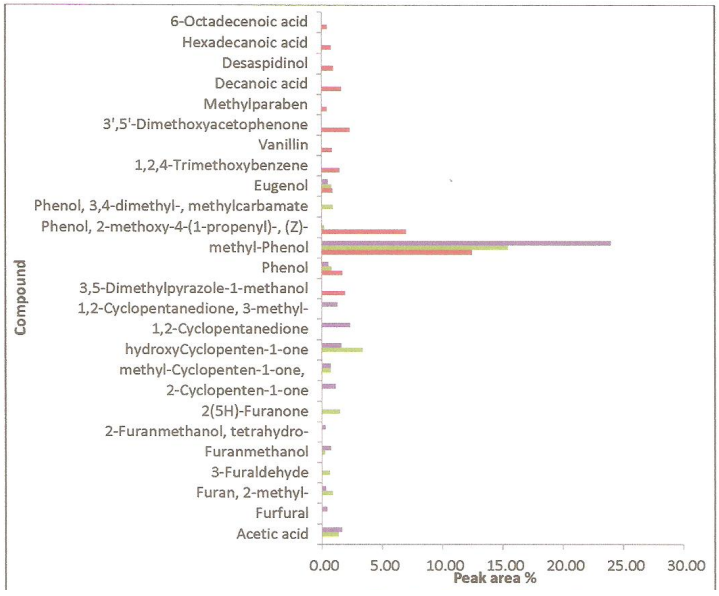

Figure 3 (b). Decomposition products from Py-GC-MS analysis of raw and torrefied *Lophira.*

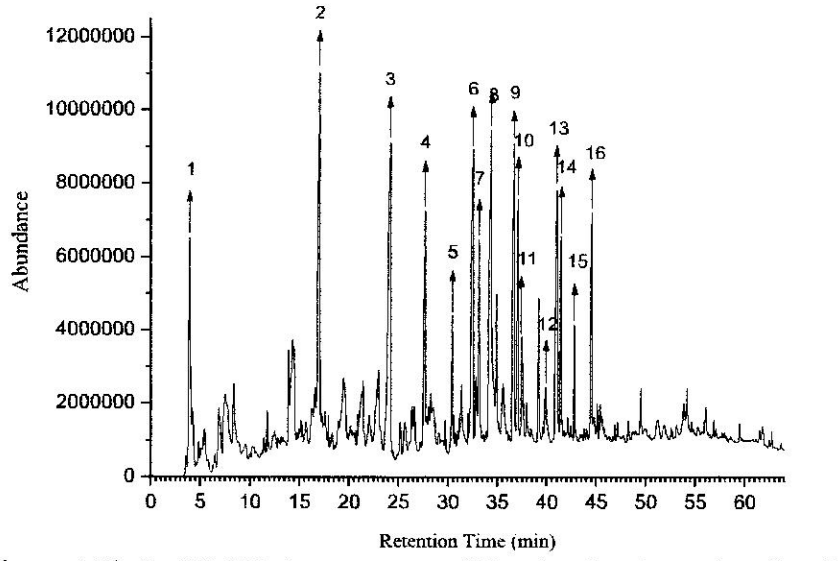

Figure S4 (a). Py GC-MS chromatogram of *Nauclea* showing assigned peaks.

The main peaks are assigned as follows: 1: 1,3-pentadiene, 2: cyclohexanol, 1-methyl4-(1-methylethenyl)-, acetate; 3: 2-methoxyphenol; 4: 2-methoxy-4-methylphenol; 5: 4-ethyl-2-methoxyphenol; 6: 2-methoxy-4-vinylphenol; 7: eugenol; 8: 2,6dimethoxyphenol; 9: 2-methoxy-4-(1-propenyl) phenol -; 10: 1,2,4-trimethoxybenzene; 11: vanillin; 12: ethanone, 1-(4-hydroxy-3-methoxyphenyl); 13: 3',5'dimethoxyacetophenone; 14&15: 2,6-dimethoxy-4-(2-propenyl)phenol.

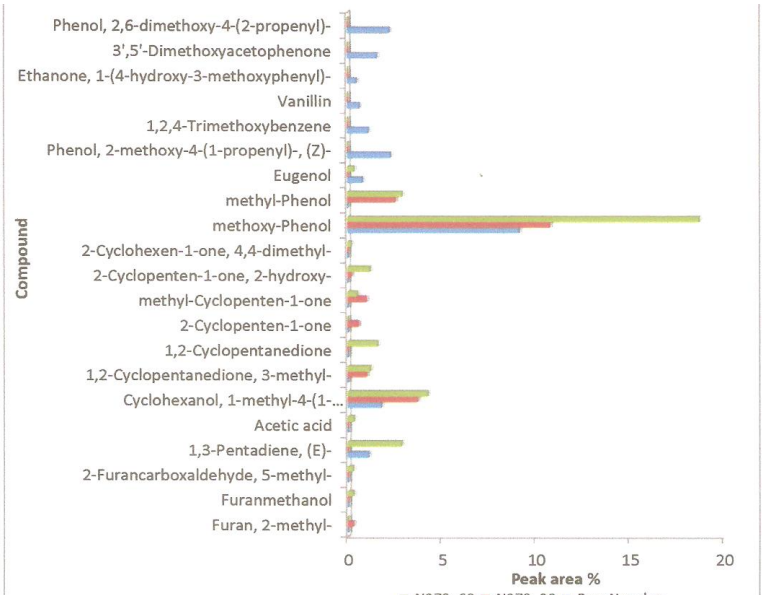

Figure S4 (b). Decomposition products from Py-GC-MS analysis of raw and torrefied *Nauclea.*

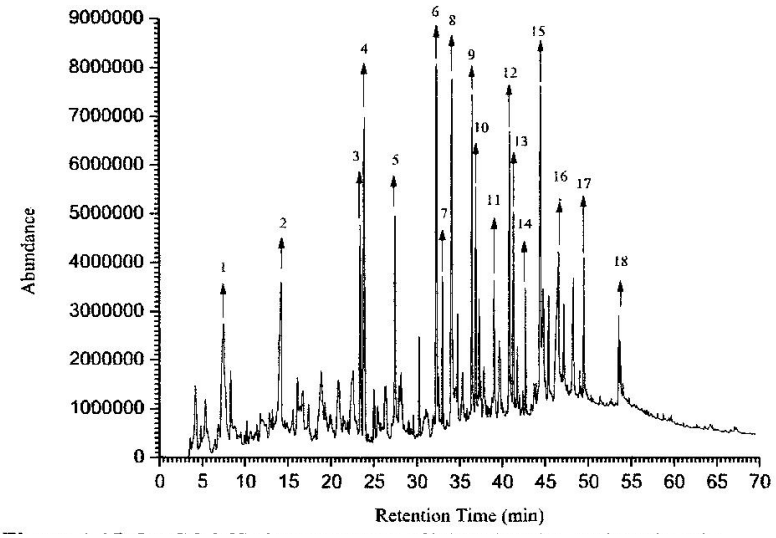

Figure 5 (a). Py GC-MS chromatogram of PKE showing assigned peaks.

The main peaks are assigned as follows: 1: furan, 2-methyl-; 2: furfural; 3: phenol; 4: 2methoxyphenol; 5: 2-methylphenol; 6: 4-methylphenol; 7: 2-methoxy-4-methylphenol; 8: 4-ethyl-2-methoxyphenol; 9: 2-methoxy-4-vinylphenol; 10: 2-methoxy-3-(2propenyl)phenol; 11: 2,6-dimethoxy-phenol; 12: 2-methoxy-4-(1-propenyl)-phenol; 13: 1,2,4-trimethoxybenzene; 14: vanillin; 15: 3',5'-dimethoxyacetophenone; 16: 2,6dimethoxy-4-(2-propenyl)-phenol; 17: n-hexadecanoic acid; 18: 6-octadecenoic acid.

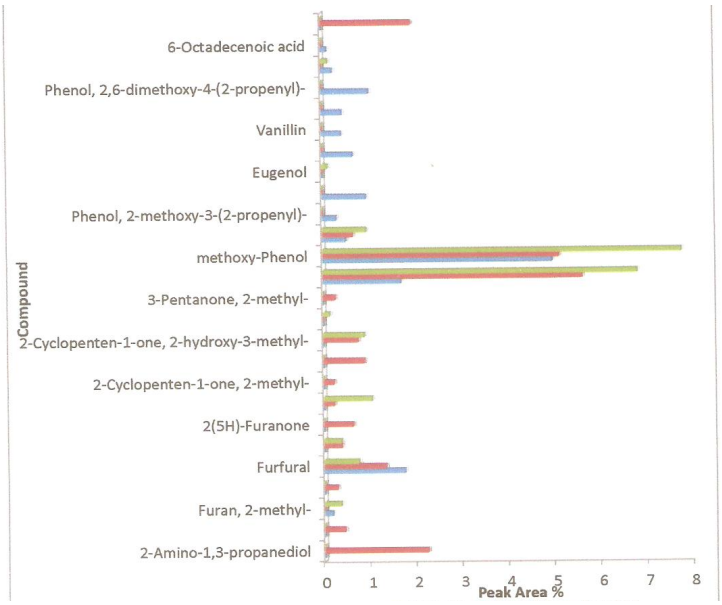

Figure S5 (b). Decomposition products from Py-GC-MS analysis of raw and torrefied PKE.